

Removal of Hexavalent Chromium Ions from Aqueous Medium using Chitosan Magnetic Nanocomposite Modified with Hexamine

Najat J. Saleh, Saad R. Sulttan , Amina J. Khazm.
Chemical Engineering Department, University of Technology

Abstract

This work integrates nanotechnology, adsorption, and magnetic separation to remove chromium (Cr) pollutant from industrial wastewater using magnetic nanoparticles. The magnetic nanocomposite consists of chitosan biopolymer and iron (Fe_3O_4) magnetic nanoparticles. The Fe_3O_4 magnetic nanoparticles were prepared by chemical co-precipitation technique and the chitosan magnetic nanocomposite (CMNC) was prepared by Ex situ process. Moreover, an amination of CMNC with hexamine to get functionalized CMNC was performed to remove Cr (VI) in wider range of pH. The prepared Fe_3O_4 magnetic nanoparticles, CMNC and functionalized CMNC were characterized using different analytical techniques, XRD, FTIR, AFM, SEM, EDX and TGA.

Batch adsorption was employed to determine the effects of pH. The adsorption results show that the functionalized CMNC possessed high activity for Cr (VI) removal in any condition of acidic, neutral and basic solutions with the percentage sorption of chromium reached to 91.7%.

Sorption isotherms were fitted with the Langmuir, Freundlich and Temkin models, it was found that the Freundlich isotherm model have the best fit with $R^2=0.998$ with functionalized CMNC. The kinetic data of Cr (VI) sorption with functionalized CMNC were fitted well with the pseudo-second order kinetic model. The reuse of the functionalized CMNC indicates that the adsorbent material is more than 80% adsorption capacity after five regeneration cycles. The results of this work shown that functionalized CMNC is a potential adsorbent to removal of Cr (VI) contaminated in a wider range of pH.

Keywords: Chitosan, Magnetic, Nanocomposite, adsorption, Hexavalent Chromium.

Paper History (Received :30-5-2018 ;Accepted :7-3-2019)

Introduction

The disposal of large quantities of wastewater due to the increase in industrial processes pollute the water with oils, metal ions, chemicals, fines and alternative materials. The presence of heavy metals ions in water bodies causes severe public health and environmental issues. Recently, hexavalent chromium component has been given due to

its negative effects, which is detrimental to human health [Hong Li, 2016, Vaishnavi S. et al., 2015].

Adsorption is one of the most important techniques used in heavy metal processing and is widely used because of the simplicity of operation and low costs. Currently nanoparticles became the most important adsorbents used in water purification because of their properties. Their applications are making easy by properties such as larger surface areas compared to bulk particles and therefore the ability to be functionalized with numerous chemical teams to extend their likeness towards target compounds [Shahriar M. et al., 2012].

Separation of pollutants by magnetic materials becomes common and fascinating in recent years. The removal of pollutants from wastewater by employing a typical adsorbent has many limitations particularly within the recollection of adsorbents when surface assimilation method, by introducing magnetic property into typical adsorbents, recollection when separation might be achieved thus simply that the lost of adsorbents might be lowered [Dong C. et al., 2014].

This work is used to remove chromium contaminants from synthetic wastewater using magnetic nanoparticles. Removal of chrome ion by magnetic nanocomposite have been published in several articles. However, most of magnetic nanocomposite were solely effective in lower pH because of the protonation of the amine groups, although Cr(VI) exists not solely within the acidic however conjointly in neutral and basic wastewater. Therefore, magnetic nanocomposite that might be applied on removal of Cr(VI) in wide range of hydrogen ion concentration was needed [Vaishnavi S. et al., 2015 ; Pooja S., & Nagendran R., 2013 ; Kyzas et al., 2009 and Khalid Z., 2010]. Functionalized of magnetic nanocomposite with hexamine groups make it positively charged at wide range of pH so that it could be applied effectively in wider range of pH.

Materials and Methods

Chitosan (molecular weight, MW=400,000, degree of deacetylation, 85%) was obtained from Sigma-Aldrich Chemicals, reagents Magnetite (Fe_3O_4), Ferric chloride (FeCl_3), and Ferrous sulfate heptahydrate ($\text{FeSO}_4 \cdot 7\text{H}_2\text{O}$) were purchased from Himedia- India. Sodium hydroxide (NaOH), Potassium dichromate ($\text{K}_2\text{Cr}_2\text{O}_7$), Ammonium hydroxide (NH_4OH) and Glacial acetic acid (CH_3COOH) were purchased from BDH-England.

Preparation of Fe₃O₄ Magnetic Nanoparticles

The Fe₃O₄ Magnetic nanoparticle preparation by chemical co-precipitation technique. 13.9 gm of FeSO₄·7H₂O dissolved in 100ml of distilled water is mixed with 27.05gm of FeCl₃ dissolved in 100ml of distilled water with constant stirring until it forms a transparent solution. Then, NH₄OH is added slowly drop by drop to the solution with continuous stirring until the pH of the solution becomes 10. A dark colored precipitate is formed at the end of reaction which is the Fe₃O₄ nanoparticles. The particles are separated using an external magnet and then dried in an oven [Jassal P. et al., 2015].

Preparation of Chitosan Magnetic Nanocomposite (CMNC)

2 gm of chitosan is dissolved in 2 vol% glacial acetic acid. The solution was sonicated for 20 minutes, and then stirred for 18 hours. 0.1 g of Fe₃O₄ nanoparticles were added to the solution and flipped again for 6 hours to obtain a chitosan–magnetite nanocomposite solution. The solution was then poured onto petriplate and allowed to dry at room temperature for 48 hours [Khalid Z. , 2010].

Functionalized CMNC with Hexamine

Amination of CMNC with Hexamine to get functionalized CMNC was performed in two steps. First, one gram of CMNC was immersed in 20 mL of methanol. 1,2-Dibromoethane (2.37 mL) was added into the mixture drop wise and the mixture was then refluxed for 24 h. The solid product was separated from the mixture using an external magnet and then washed with ethanol and dried in an oven at 40°C for 12 h. Next, the solid product resulted from the first step was immersed in 20 mL methanol and hexamine (0.83 gm) was added to the mixture and then was refluxed for 12 h under continuous stirring. Finally the obtained product was separated with an external magnet, washed with ethanol and deionized water for several times and dried in an oven for 24 h at 40 °C.

Adsorbent Characterization

The prepared magnetic nanoparticle and the CMNC samples were characterized using different analytical techniques by X-Ray diffraction– Shimadzu-6000, Origin: Japan, Fourier transform infrared spectroscopy– Perkin Elmer Spectrum FTIR instrument, atomic force microscope–Park AFM XE-100 a Zeiss Supra 35VP, SEM EDX instrument and thermogravimetric analyzer TGA/DTA (Perkin Elmer TGA7). Heavy metal ion analysis were done using Atomic absorption spectrometry (AA-6300, Germany).

Batch Adsorption Experiments

So as to describe the sorption behavior of Cr onto CS, CMNC and functionalized (CMNC) in aqueous phase, a

single component sorption experiments were conducted employing K₂Cr₂O₇ as a representative of Cr. The standard solutions that contain (10, 20, 30, 40, 50, 60 and 70) mg/L of Cr(VI) using K₂Cr₂O₇ from stock solutions using dilution method.

Adsorption Isotherms

The experimental adsorption isotherm for Cr(VI) removal was performed at room temperature (25 ±2°C) using synthesized samples of functionalized CMNC. Adsorption isotherms were obtained at pH 5 by mixing 20 mL of Cr(VI) solutions of different concentrations (10, 20, 30, 40, 50, 60 and 70 mg/l) with amount of the two synthesized 0.1 g of were previously sealed and closed, and the suspensions were stirred by electrical water bath shaker [Type: BS-21, Origin: Germany] at 200 rpm. The amount of Cr(VI) adsorbed was calculated by subtracting the amount found in the liquid after adsorption from the amount of Cr(VI) existing before the addition of the adsorbent by atomic absorption spectrometry (AAS). The adsorption data for Cr(VI) was fitted to Langmuir, Freundlich and Temkin isotherms represented by equation 1, 2 and 3.

Kinetic and Intraparticle Diffusion Models

The adsorption kinetics experiments by using functionalized CMNC were performed in conical flasks containing 20 ml of Cr(VI) solution of 10,20,30,40,50,60,70,mg/l concentration and pH 5-9. A 0.1 g and functionalized CMNC was added to the flask at room temperature (25 ± 2°C). The mixture was stirred by electrical shaker at 200 rpm. An equilibrium study was performed by taking the sample for analysis at regular intervals from 10 To 300 min.

The adsorbent was separated for the short-time experiments to avoid potential interference from suspended scattering particles in the atomic absorption spectrometry (AAS). The rate of sorption was calculated using three kinetic models, namely pseudo-first-order, pseudo-second-order and Intraparticle diffusion.

Sorption Thermodynamics

The thermodynamic parameters for the sorption of chromium on functionalize CMNC at different temperatures (30, 50, 70 °C) were performed in conical flasks containing 20 ml of chromium solution of 30 mg/l concentration and pH (5-9). A 0.1 g CS and 0.1 and functionalized CMNC was added to the flasks. The solution was mixed by electrical shaker at 200 rpm. An equilibrium study was performed by taking the sample from the shaker at 200 min.

Regeneration of adsorbent

The recovered adsorbent was rinsed after the batch balance studies with moderate distillation to remove the remaining Cr(VI) particles and then dry them. The dried

sorbent was placed in a solution containing 200 ml of 0.1 M NaCl for 2 hours. This cycle was repeated for five times.

Results and Discussion

Characterization of Fe₃O₄ Magnetic Nanoparticles

The structural analysis of prepared Fe₃O₄ magnetic nanoparticles was checked by using X-ray diffractometer (XRD) and the results are shown in **Fig. 1**. The XRD of

Fe₃O₄ magnetic nanoparticles show six characteristic peaks of Fe₃O₄ confirming that the resultant nanoparticles consists of Fe₃O₄ with a spinel structure. The results showed that the coating process did not change in the Fe₃O₄ phase. The peaks corresponding to (hkl) values of (220), (311), (400), (422), (511) and (440) located at 30.22, 35.56, 43.22, 53.70, 57.12 and 62.72 degrees were characteristic of Fe₃O₄ with a face-centred-cubic structure. The result obtained in the present study are in good agreement with those obtained by [Peng W. et al.,2013].

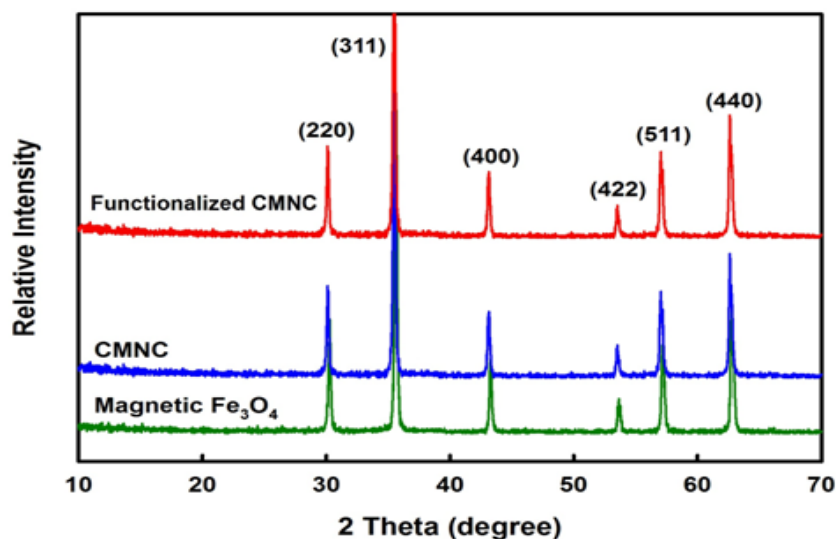


Fig. 1 X-ray diffractometer of magnetic Fe₃O₄, CMNC and functionalized CMNC.

The XRD structural analysis of chitosan magnetic nanocomposite (CMNC) and functionalized CMNC are shown in **Fig. 1**. The results show the same six characteristic peaks of Fe₃O₄ confirming that the resultant nanoparticles consist of Fe₃O₄. The results showed that the coating process did not change in the Fe₃O₄ phase. These results are consistent with what has already been reported magnetite chitosan prepared by different methods [Thinh N. et al.,2013; Peng W.,2013]. In comparison with Fe₃O₄ magnetic nanoparticles, the diffraction peaks of CMNC and functionalized CMNC have no significant difference. It means that there is no change in the structure of Fe₃O₄ during functionalization with hexamene.

Fig. 2 a shows the result of the FTIR analyses of prepared Fe₃O₄ magnetic nanoparticles by chemical co-precipitation technique. It is illustrated that the strong absorption band at 586 cm⁻¹ is due to Fe–O bond vibrations, which prove the Fe₃O₄ nanoparticles formation. Many researches were description the

characteristic absorption of Fe–O band in Fe₃O₄ be at 586 cm⁻¹. Also, the result is in agreement with the result obtained by [Waldon R., 2008; Dong W. et al., 2012; Peng W., 2013a].

FTIR was analyzed for the chitosan magnetic nanoparticles (CMNC) and functionalized CMNC are shown in **Figs. 2 b & c**. It is illustrated by the figure that the addition of chitosan to the nanoparticles show the peak of iron with the peaks of the original chitosan, which consists of 3327.36 cm⁻¹ for O–H bond stretching N–H bond stretching, 2926 cm⁻¹ for C–H stretching, The band at 1246 cm⁻¹ can be attributed to C–N stretching vibration and the band at 1016.34 cm⁻¹ to the stretching vibration mode of the hydroxyl group., 1653 cm⁻¹ for C=O of NH=C=O bond stretching, 601cm⁻¹ for Fe–O group due to pure Fe₃O₄. As for the functionalized CMNC, it turned out that the peaks of the amin was more pronounced because of its presence in hexamine. These results are in agreement with previously reported by [Jucély D. et al., 2015; peng w., 2013].

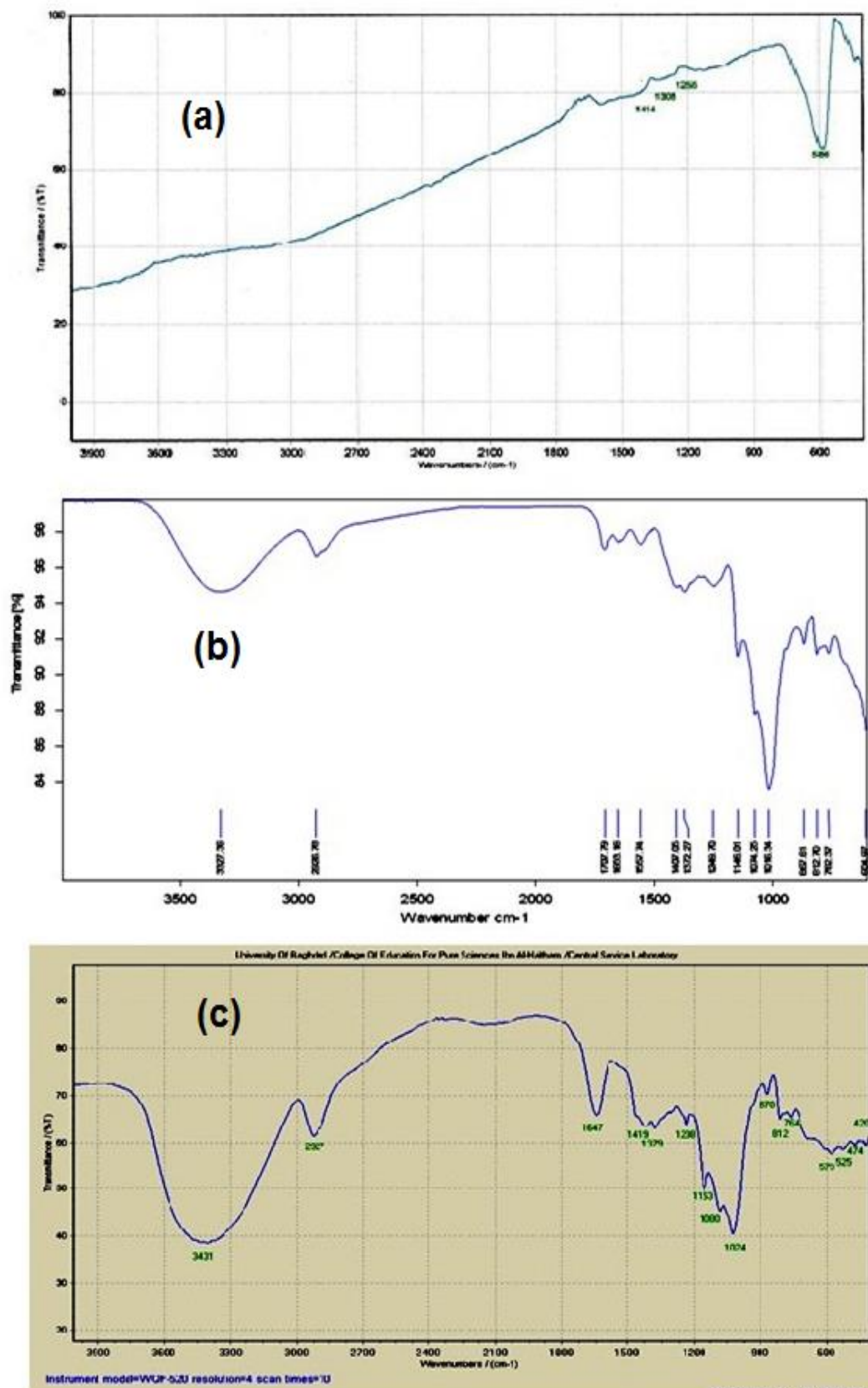


Fig. 2(a) The infrared spectrum of Fe₃O₄ magnetic nanoparticles. (b) The infrared spectrum of CMNC. (c) The infrared spectrum of functionalized CMNC.

The surface morphology and the diameter of prepared Fe₃O₄ magnetic nanoparticles were studied using Atomic Force Microscope (AFM), both two and three-dimensional images of magnetite nanoparticles Fe₃O₄ were obtained as shown in Fig. 3. The properties of magnetite nanoparticles by AFM have revealed that particle sizes are evenly distributed and particle size was found to be around (65–90 nm) and the average diameter

of (77.13 nm). The three dimensional surface image shown in Fig. 3 confirms that Fe₃O₄ magnetic nanoparticles are spherical in shape and agglomerated in form. Table 1 and Fig. 4 show the particle size distribution of Fe₃O₄ magnetic nanoparticles. The results obtained confirm that the most volume percentage 25.23 % of particle size distribution was at 70 nm and the lowest volume percentage 0.46 % was at 120 nm.

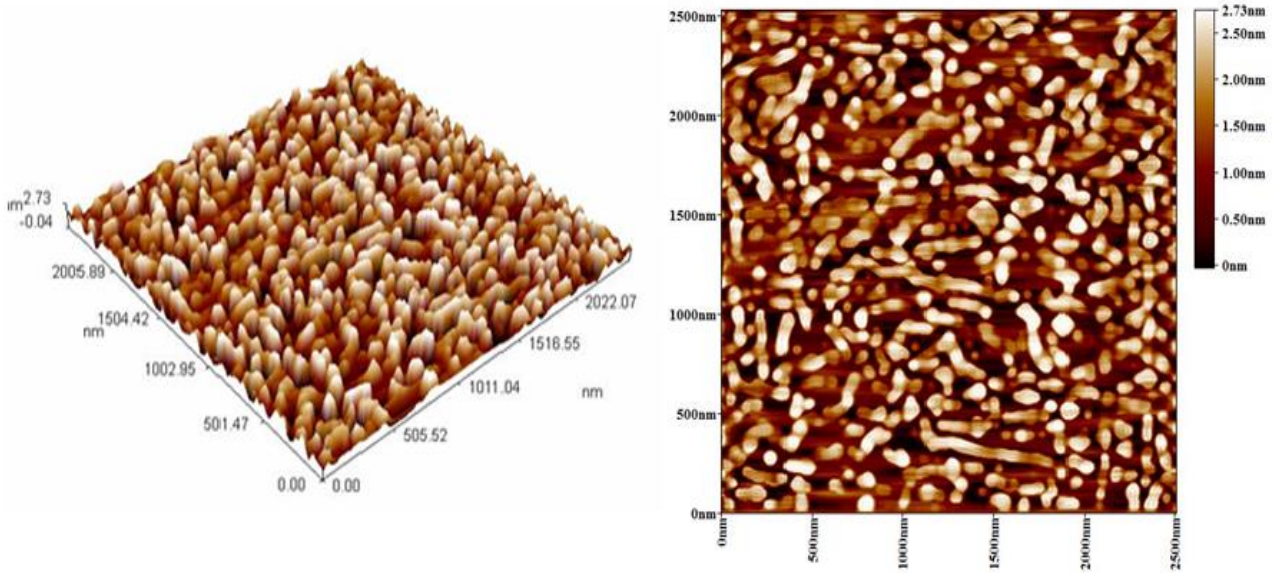


Fig. 3 AFM Three-dimensional surface profile for Fe₃O₄ magnetic nanoparticles.

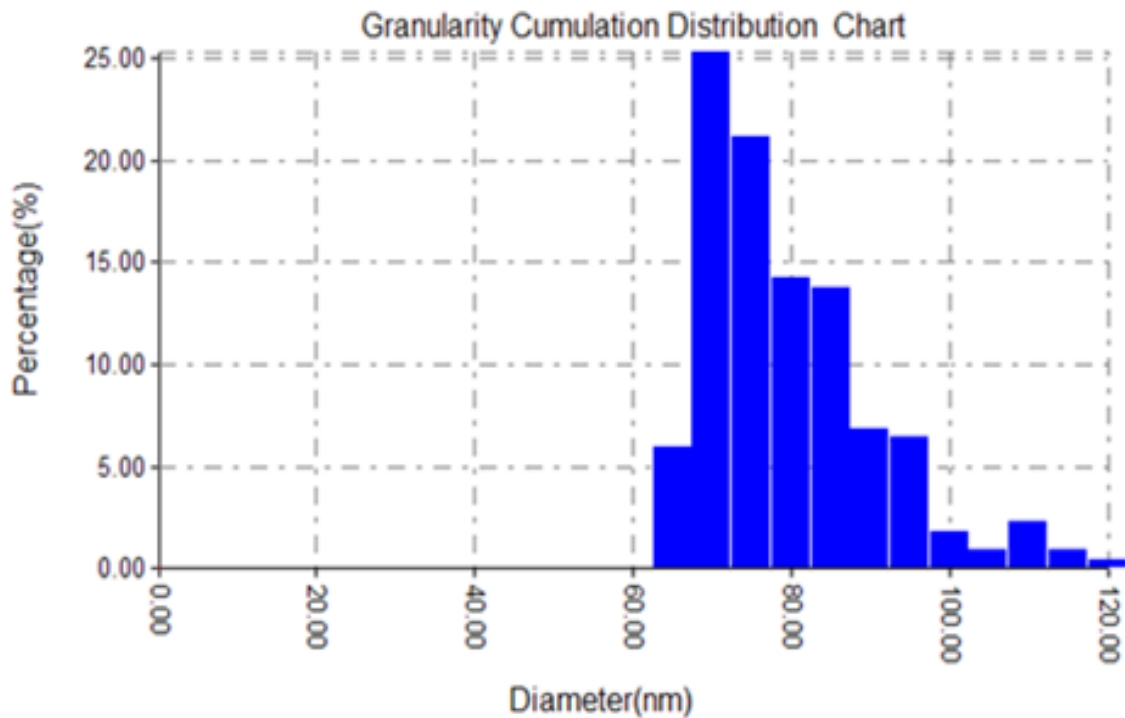


Fig. 4 Bar chart of particle size distribution of Fe₃O₄ magnetic nanoparticles.

Table 1. Particle size distribution of Fe₃O₄ magnetic nanoparticles with average diameter of 77.13 nm

Diameter(nm)<	Volume (%)	Cumulation(%)	Diameter(nm)<	Volume (%)	Cumulation (%)	Diameter (nm)<	Volume(%)	Cumulation (%)
65.00	5.96	5.96	85.00	13.76	80.28	105.00	0.92	96.33
70.00	25.23	31.19	90.00	6.88	87.16	110.00	2.29	98.62
75.00	21.10	52.29	95.00	6.42	93.58	115.00	0.92	99.54
80.00	14.22	66.51	100.00	1.83	95.41	120.00	0.46	100.00

Surface morphological images obtained by SEM and the energy dispersive X-ray (EDX) for the Fe₃O₄ magnetic nanoparticles as described in Fig. 5. It can be observed that the particles between 60-100 nm are almost in spherical shape. The collected particles appear, this probably as a result of Fe₃O₄ magnetic nanoparticles being a hydrophobic surface, and due to hydrophobic interaction between the particles, which causes the particle to agglomerate and form large clusters. The Fe₃O₄ magnetic nanoparticles EDX spectrum confirms the composition of iron (69.8%) and oxygen (30.2%). Also, the result is in consistent with those obtained by [Katayoon K. et al., 2014].

the Fe₃O₄ nanoparticles are dispersed in the functionalized CMNC. The number and energy of the X-rays emitted from a specimen can be measured by an energy-dispersive spectrometer. The EDX analysis of these particles indicates the existence of iron and oxygen and carbon composition in the functionalized CMNC. The component composition of oxygen, carbon and iron is 38.4, 31.1 and 30.5%, respectively. The nitrogen element is not detected because it is available at a lower rate than the rest of the elements and the nature of the device is not sensitive to nitrogen if it is not in large proportions, these results are in agreement with previously reported by [Vaishnavi S. et al., 2015].

A typical SEM and EDX images for the functionalized CMNC shown in Fig. 6. The SEM image explained that

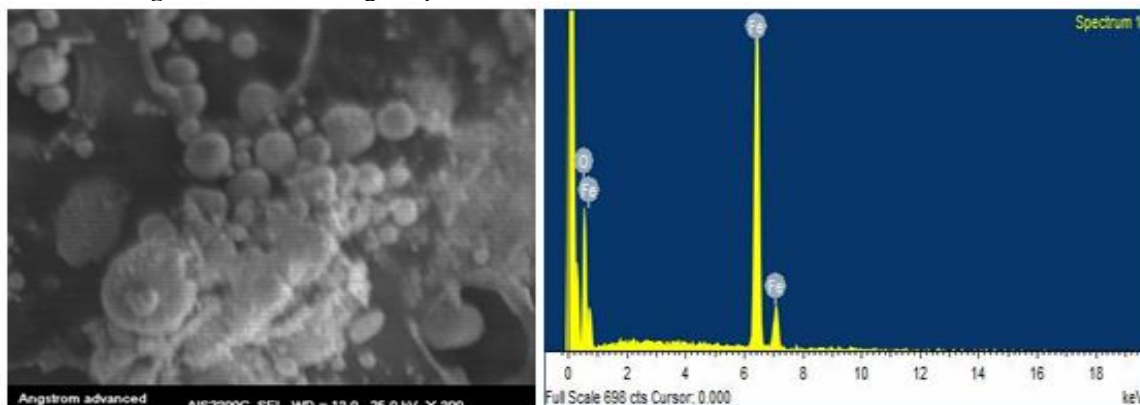


Fig. 5 SEM-EDX images for Fe₃O₄ nanoparticles.

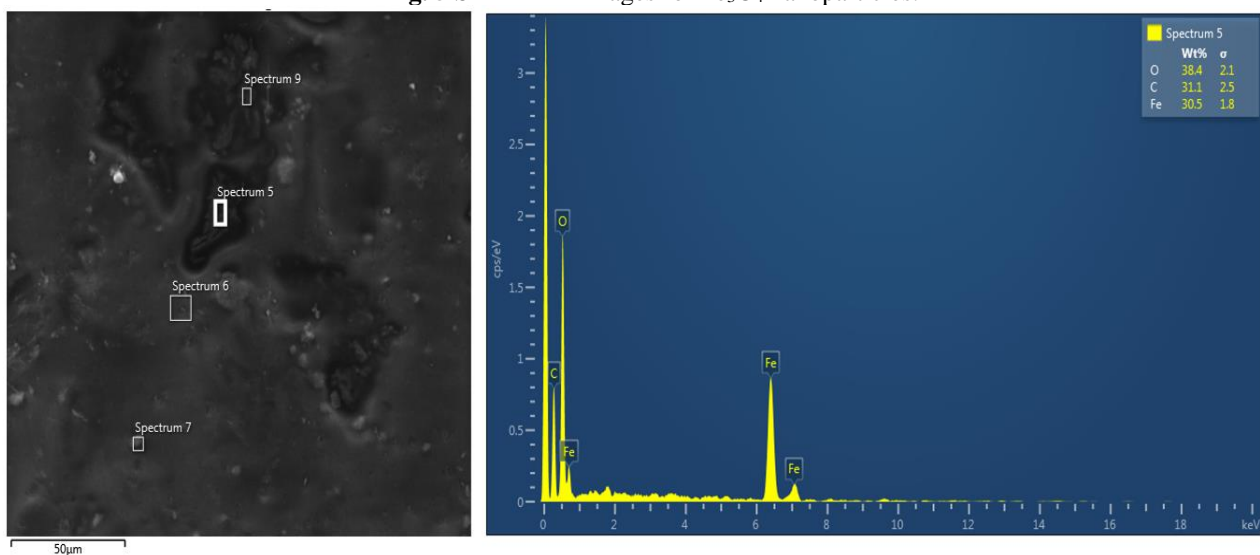


Fig. 6 SEM-EDX images for functionalized CMNC.

Thermo gravimetric analysis (TGA) curves for the functionalized CMNC is presented in Fig. 7. The curve in the blue line depicts the change in the weight of the sample in percentage with temperature. Three steps weight loss was observed. The first step from 50 °C to 131.8 °C (1 wt %) can be attributed to the loss of moisture from the sample structure. The second weight

loss observed at 131.8 °C to 301.2 °C (44 wt %) is due to the degradation of functionalized CMNC, while the third weight loss between 301.2 °C to 569.3 °C (76 wt %) can be attributed to the decomposition of the functionalized CMNC main chain. The total weight loss is 77.91% at 585.48 °C. These results are in agreement with previously reported by [Jucely d. et al., 2015].

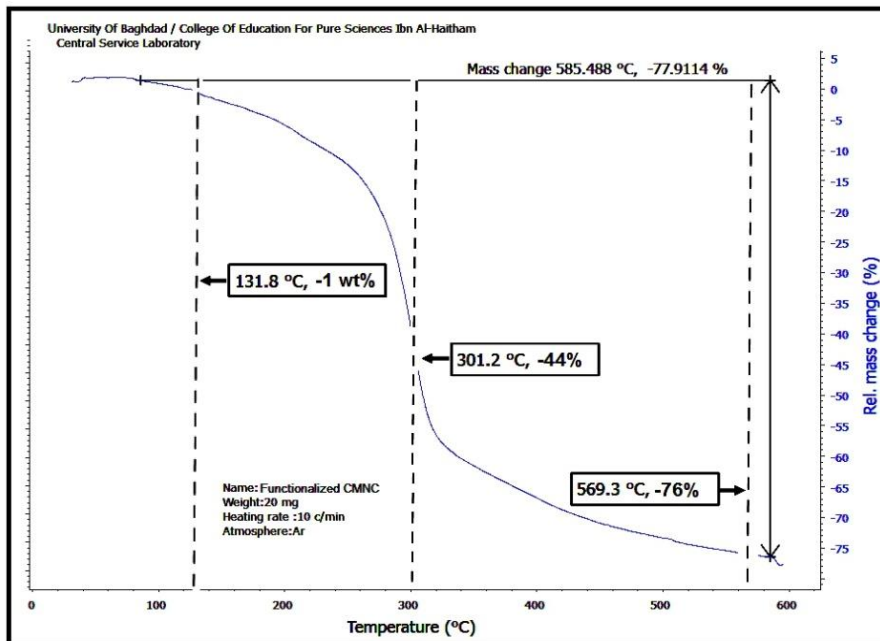


Fig. 7 Thermo-gravimetric analysis of functionalized CMNC.

Batch sorption

Comparison of the three adsorbents

A comparative study was carried out between the three tested adsorbents in order to investigate the effectiveness

of functional group of chitosan (CS), chitosan magnetic nanocomposite (CMNC) and functionalized CMNC on the sorption of chromium from its aqueous solutions. Fig. 8 showed the chromium sorption for Chitosan (CS), Chitosan magnetic nanocomposite (CMNC) and Functionalized CMNC at various pH values.

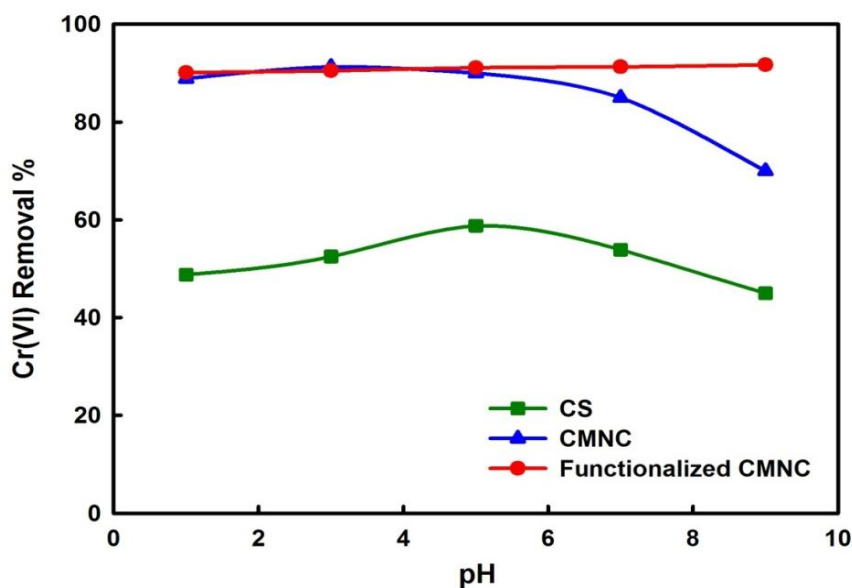


Fig. 8 The effect of pH value on % Cr(VI) removal using Chitosan (CS), Chitosan magnetic

nanocomposite (CMNC) and Functionalized CMNC adsorbents at initial concentration= 30 mg/l, adsorbent dose= 0.1gm,contact time= 200 min.

From this Figure, it is clearly that the highest percentage sorption of Chromium by chitosan was observed at pH= 5 with increase in pH from 1 to 9 the percentage sorption of chromium decreased from 58.8% to 48.8% , there are still some limitations in the application of the chitosan based materials because chitosan can be applied only in the acidic solution where $-NH_2$ groups of chitosan are protonated. As pH increased, amine groups become less active towards Cr(VI). While the Fe_3O_4 is coated with chitosan (CMNC), the percentage removal increases to 94.5 % in the acidic medium. However, in case of addition of hexamine and at the basic medium, the percentage sorption of Chromium reached 91.7% at pH= 9.

3.3.2. Effect of Sorbent Dose

Experiments were done to establish an appropriate sorbent Chitosan (CS) and Functionalized CMNC) dose for Chromium removal with the results shown in **Fig. 9**. From the figure it seem that by increasing the dosage of sorbent the removal ratio increases as a result of increasing surface area of adsorption. The percentage of chromium removed increased from 16 to 58.8 % with increasing the dosage from 0.02 to 0.1 g of chitosan, While increasing in the dosage from 0.02 to 0.1 g of functionalized CMNC, the percentage of chromium removed increased from 51.6 to 91.7 %. This dosage agreement with [Auta M. and Hameed B., 2014; Dong W. et al., 2012].

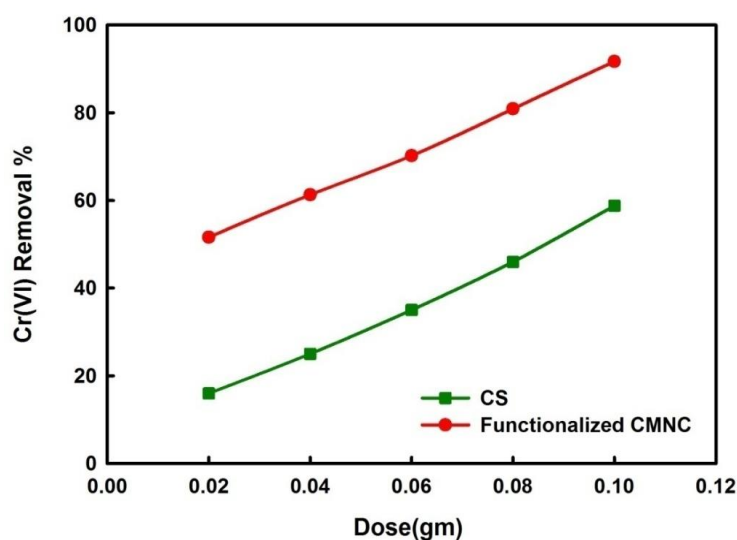


Fig. 9 Effect of Chitosan (CS) and Functionalized CMNC Dose using ($Co=30$ mg/l, 298 K, contact time= 200 min and r.p.m=200).

Effect of Contact Time

The effect of contact time for removal of Chromium by the chitosan (CS) and Functionalized CMNC as is shown in **Fig. 10**. From figure we note that, the rate of the chromium is rapid adsorption in the first 50 min and, thereafter, the adsorption rate increased gradually and the

adsorption reached equilibrium at 200 min for CS and 150 min for Functionalized CMNC. Increasing the contact time up to 200 min showed that the chromium removal increased by 58.8% over those obtained at 200 min , while in functionalized CMNC adsorption reached equilibrium at 150 min and this agreement with those of [Hua Y. et al., 2010; George Z. et al., 2013].

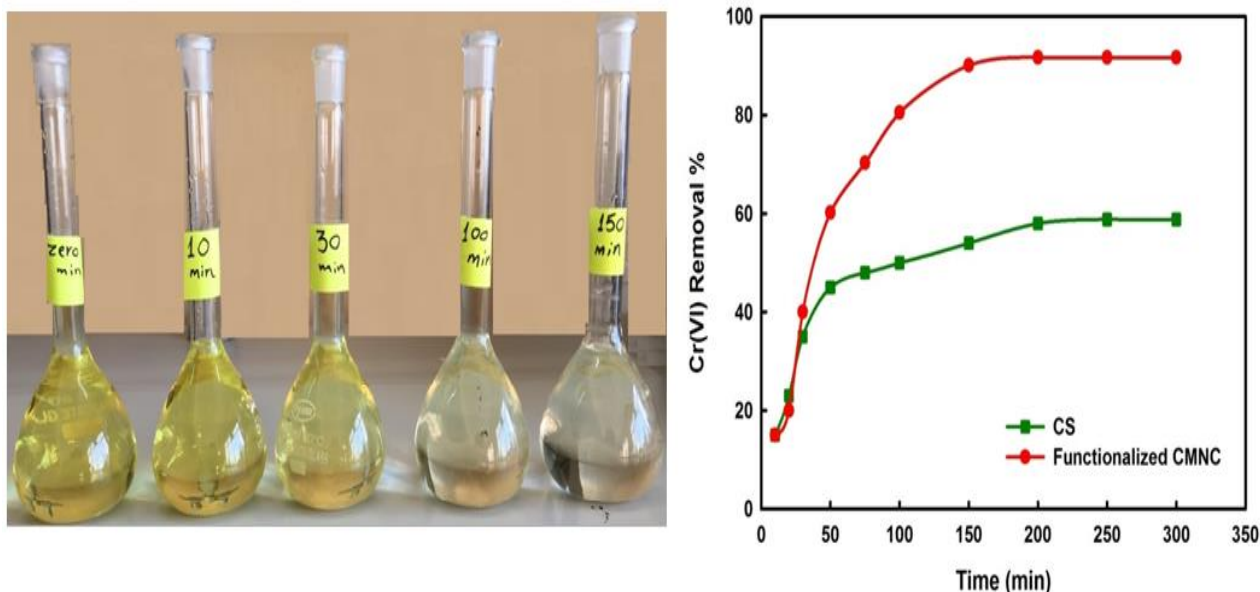


Fig. 10 Effect of contact time on adsorption of Cr(VI) by the chitosan (CS) and functionalized CMNC using ($C_0=30$ mg/l, adsorbent dose=0.1gm, 298 K, and rpm=200).

Effect of Initial Chromium Concentration

The effect of initial chromium concentration on the removal of chromium by chitosan and functionalize CMNC is shown in **Fig. 11**. From figure we note that, the amount of sorbed chromium per unit mass of chitosan and functionalized CMNC (q_e) increased with increasing the initial concentration of chromium C_0 from 10 mg/L to 70

mg/L, although the percentage chromium removal decreased with the increase in the initial concentration of chromium. The initial concentration provides necessary driving force by the concentration gradient ($\Delta C=C_0-C_e$) to overcome the resistance to the mass transfer of chromium between the aqueous and the solid phases. This result was in a good agreement with the finding of [Nguyen N. et al., 2012; Xin j. et al., 2010].

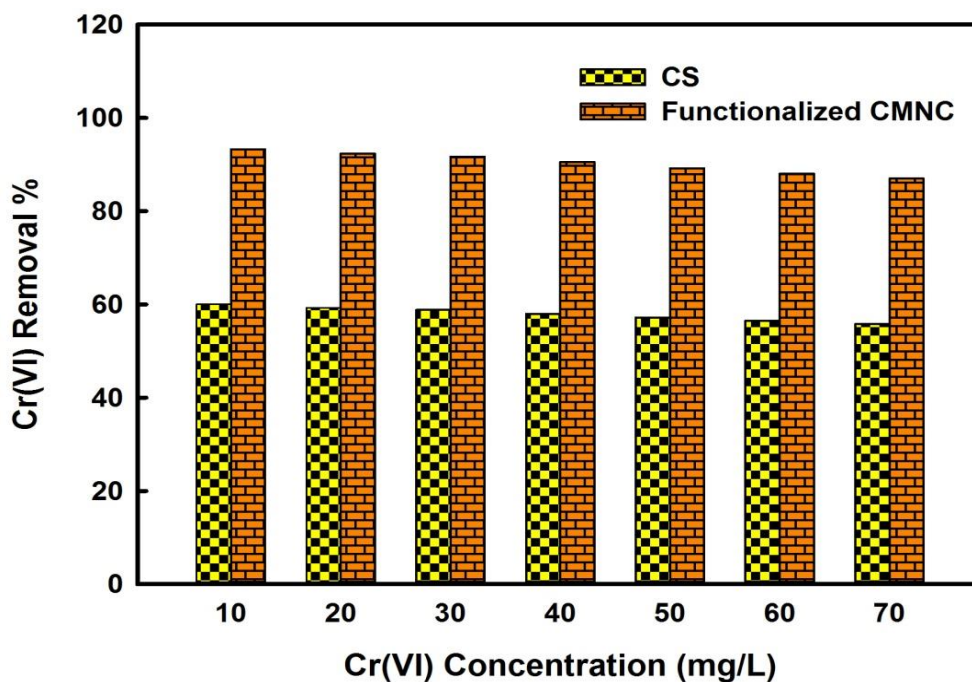


Fig. 11 Effect of initial Chromium concentration on the amount of chromium adsorbed by chitosan(CS) and functionalized CMNC using ($C_0=30$ mg/l, adsorbent dose=0.1gm, 298 K, and r.p.m=200).

Effect of Temperature

The effect of temperature on the removal of Chromium by chitosan(CS) and functionalized CMNC at 30, 50, and 70°C is shown in **Fig. 12**. There is no change in removal rate was noted (58.8, 62.4, and 66.23%, respectively) for chitosan and (94.5, 95.6 and 96.7%, respectively) for

functionalized CMNC, materials can be utilized in ambient temperature, thus reducing the energy costs of processes used to remove environmental contaminants. This outcome is in a good agreement with the results noted by [Peng w. et al., 2013].

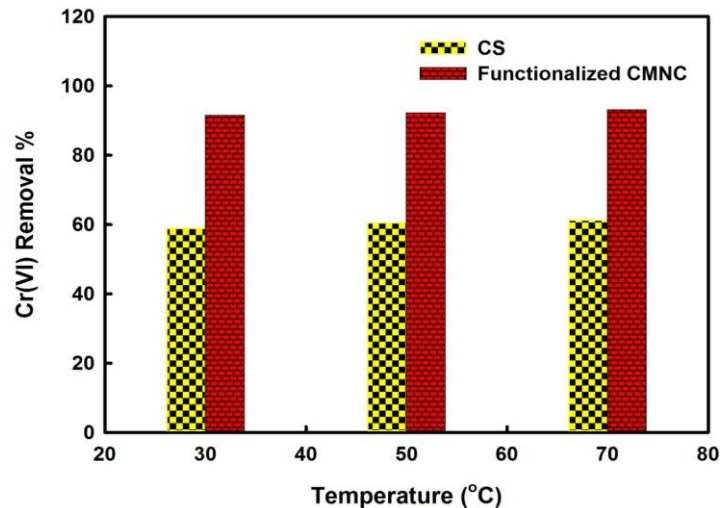


Fig. 12 Effect of temperature on adsorption of Chromium by 0.1g chitosan(CS) and functionalized CMNC using ($C_0=30$, adsorbent dose=0.1gm, time=200min, r.p.m=200).

Equilibrium adsorption isotherm studies

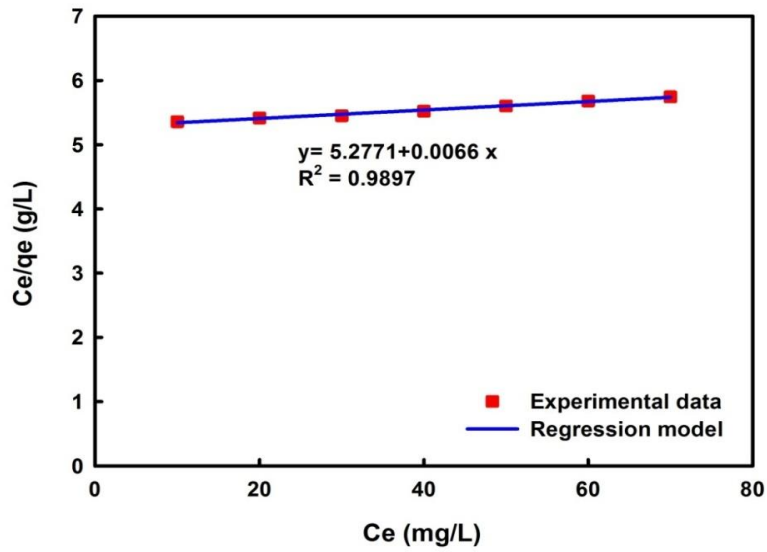
In order to indicate the behavior of sorption capacity of functionalized CMNC, sorption isotherms have been studied by three linearized isotherm models, Langmuir [Langmuir, 1916], Freundlich [Freundlich, 1906] and Temkin [Temkin and Pyzhev, 1940]. The isotherm models fitting to the experimental data were carried out using their non-linear equations expressed as:

$$q_e = \frac{q_{\max} b C_e}{1 + b C_e} \quad \text{Langmuir model} \quad (1)$$

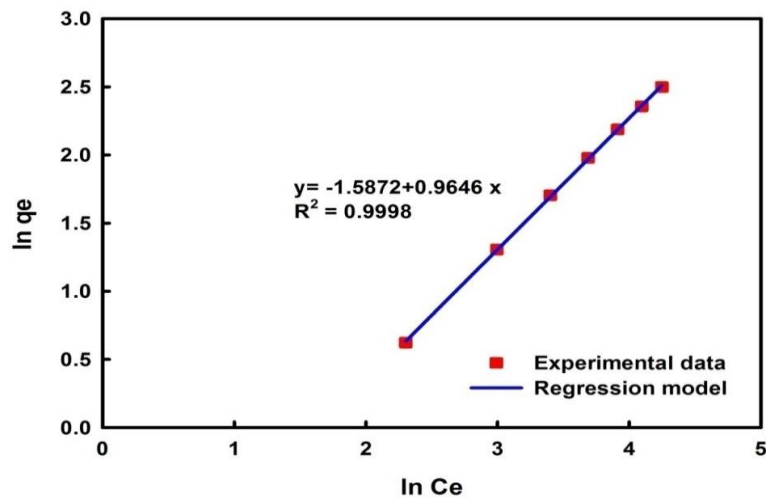
$$q_e = K_f C_e^{1/n} \quad \text{Freundlich model} \quad (2)$$

$$q_e = \frac{RT}{b_T} \ln K_T C_e \quad \text{Temkin model} \quad (3)$$

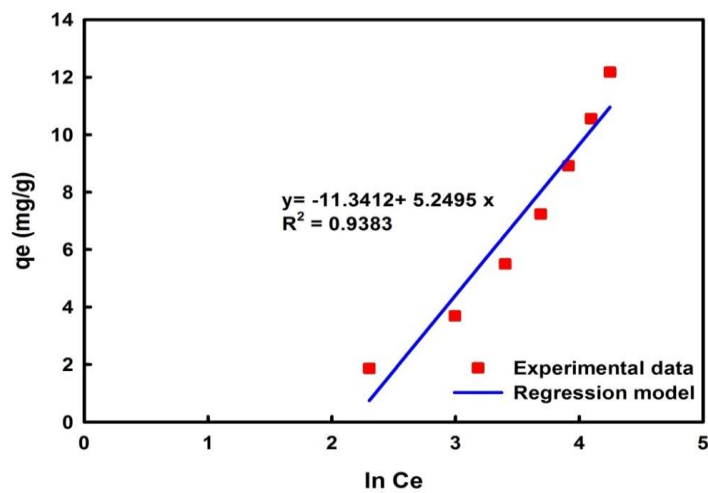
Where C_e (mg/L) and q_e (mg/g) are the equilibrium concentration and the amount of Cr(IV) adsorbed, respectively; q_{\max} (mg/g) and b (L/g) are the monolayer adsorption capacity and affinity of functionalized CMNC towards chromium, respectively. The K_f ((mg/g) (L/mg)^{1/n}) and n (dimensionless) are the Freundlich constants relaying information on the adsorption extent and degree of nonlinearity between the adsorption and the solution concentration, respectively. K_T the Temkin equilibrium binding constant (L/g) corresponding to the maximum binding energy, b_T is Temkin isotherm constant and is related to heat of sorption (KJ/mol), R is the universal gas constant (8.314 J/mol K), and T is absolute temperature (K), sorption isotherms have been studied for three linearized isotherm models (Langmuir, Freundlich and Temkin) at 298 K. Plots are given in **Fig. 13**



(a)



(b)



(c)

Fig. 13 (a) Langmuir Isotherm model for functionalize CMNC
(b) Freundlich Isotherm model for functionalize CMNC.
(c) Temkin Isotherm model for functionalize CMNC.

The models parameters and the correlation coefficient (R^2) for each model obtained are summarized in **Table 2**. It can be seen from this Table that the coefficient of determination values for Langmuir model, $R^2= 0.9897$, was obtained and that's acceptable results. Freundlich

Isotherm model, $R^2= 0.9998$ were obtained and that's a good agreement.

The Temkin Isotherm model, $R^2= 0.9383$ were obtained and that's agreement. The high R^2 values (0.999) of Freundlich isotherm indicates that the adsorption follow Freundlich model more than the other two models used.

Table 2: Model parameters for the sorption of Chromium.

Adsorbent	Langmuir					Freundlich			Temkin		
	T(K)	q_{max} (mg/g)	b(l/mg)	R^2	R_L	K_f (mg/g)	n	R^2	K_T (l/g)	b_T (KJ/mol)	R^2
functionalize CMNC	298	151.51	0.00125	0.989	0.963	0.20	1.03	0.999	0.11	5.24	0.938

Kinetic of sorption

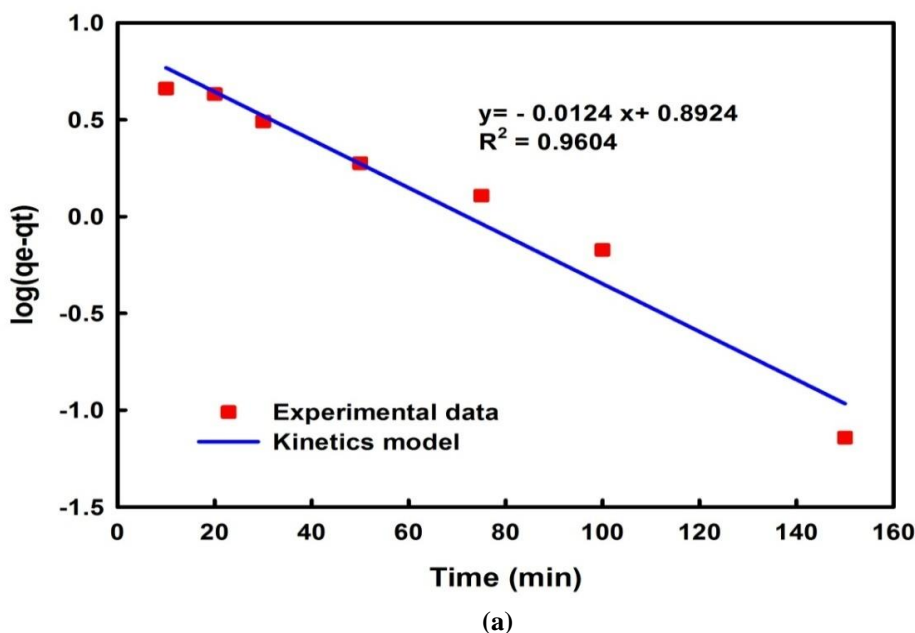
The kinetic experiment data were modeled by pseudo-first-order and pseudo-second-order kinetic equations. The nonlinear expressions of the models are expressed as:

$$q_t = q_e(1 - e^{-k_1 t}) \quad \text{for pseudo 1order} \quad (4)$$

$$q_t = \frac{k_2 q_e^2 t}{(1 + k_2 q_e t)} \quad \text{for pseudo 2order} \quad (5)$$

Where q_e and q_t (mg/g), are the amount of chromium adsorbed at equilibrium and at any time t (min), respectively; k_1 (h^{-1}) and k_2 (g/mg h) are the pseudo-first-order and pseudo-second-order rate constants, respectively.

The kinetics of the chromium sorption on functionalized CMNC was screening by using pseudo-first and second order kinetics models as shown in **Fig. 14**



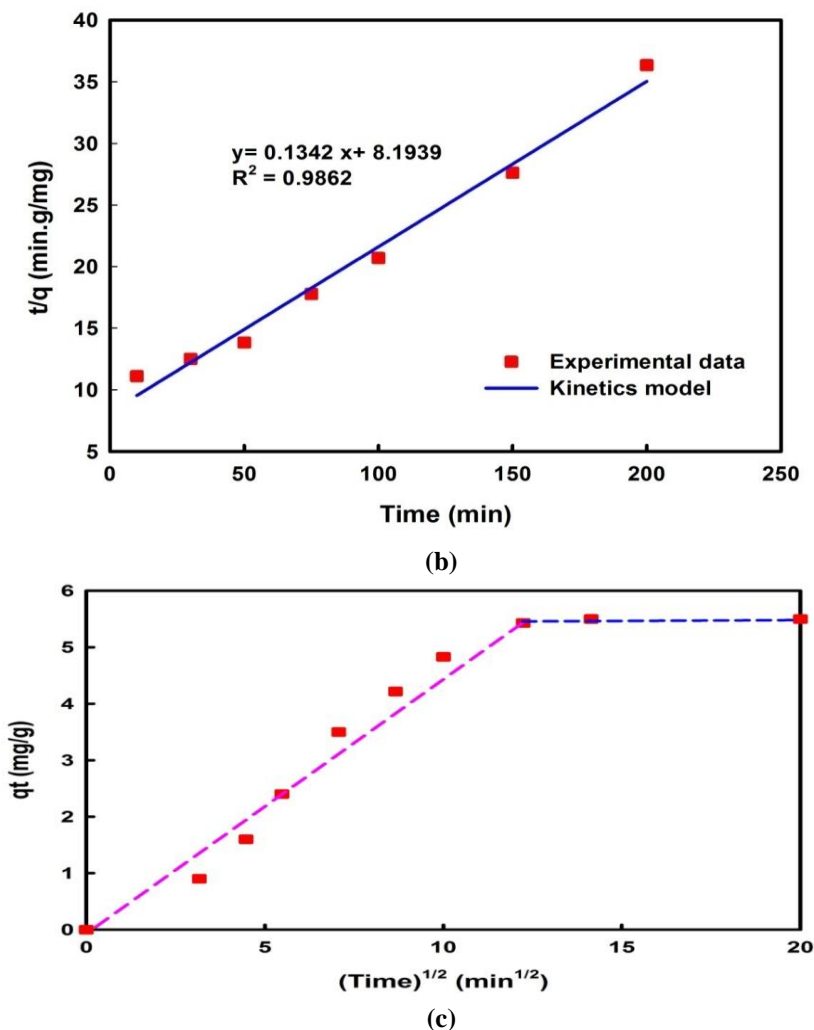


Fig. 14 (a)Pseudo-first order kinetics model for functionalize CMNC. (b) Pseudo- second order kinetics model for functionalize CMNC. (c)Intraparticle Diffusion model for functionalized CMNC.

The plot of values of qt vs. t was used to determine the q_e and k_1 parameters which shown in **Table 3**. The results showed that the second-order model has the best

fit for experimental data. This was observed by a high correlation coefficient (R^2) of 0.9862.

Table (3): Pseudo-first order and pseudo-second order kinetic models for the sorption of chromium on the functionalized CMNC.

Adsorbent	Pseudo- first order					Pseudo- second order		
	T(K)	$q_{exp}(mg/g)$	$q_{calc}(mg/g)$	$K1(min^{-1})$	R^2	$q_{calc}(mg/g)$	$K_2 (g/mg.min)$	R^2
functionalize CMNC	298	5.502	7.805	0.0285	0.9604	7.451	0.00219	0.9862

Sorption Thermodynamics

The adsorption process of functionalized CMNC and Cr(VI) equilibrium surface interaction was studied by adopting Gibb’s expression over temperature range of 30 - 50 °C. The Gibb’s free energy (ΔG) of the process was determined using the following equation:

$$\Delta G = -RT \ln K_c \tag{6}$$

And the enthalpy (ΔH) and entropy (ΔS) of activation the Cr(VI) adsorption were determined from free energy equation :

$$\ln K_c = \frac{\Delta G}{RT} = \frac{\Delta S}{R} - \frac{\Delta H}{RT} \tag{7}$$

Where R is the universal gas constant (8.314 J/Kmol); T, absolute temperature (K); K_c distribution coefficient expressed as $K_c = q_e / C_e$ (adsorbent)/ C_e (solution), and from the plot of $\ln K_c$ against $1/T$, the intercept and

slope were used to determine values of ΔH and ΔS , respectively, intraparticle diffusion model was applied to the experimental data as shown in Fig. 15 and the

thermodynamic adsorption parameters determined are summarized in Table 4.

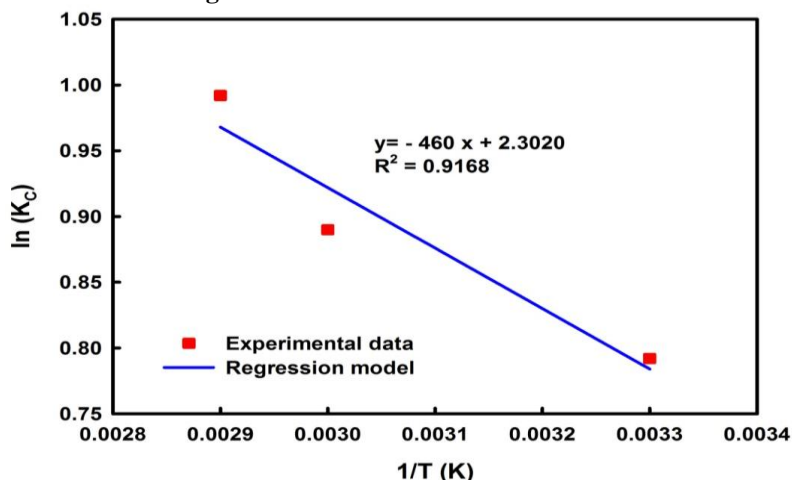


Fig. 15 Ln Kc vs. 1/T plot for chromium sorption by functionalized CMNC.

It is noted from the figure that the positive values of ΔG were positive indicating that the total Cr biosorption process not spontaneous and therefore requires some energy from an external source in order to occur. [Dogan M.et

al.,2009], while the positive value of enthalpy ΔH indicates that the sorption is endothermic. ΔS were positive indicating that the increased randomness at the solid solution interface during the fixation of adsorbents on the active sites of the adsorbent.

3.3.9. Regeneration of Functionalized CMNC

The reuse of an adsorbent is important property for practical applications. In this study, a mixture of the solution of 0.1 mol/L NaCl was used as regeneration desorption agent. Fig. 16 show the five reusability cycles of functionalized of CMNC. It can be seen that a slightly decreased in adsorption efficiency with cycle increased and remained almost constant for the first three cycles. These results show that the functionalized CMNC can be used as a reusable for Cr adsorption from aqueous; this result was in a good agreement with the finding reported by [Peng W., 2013].

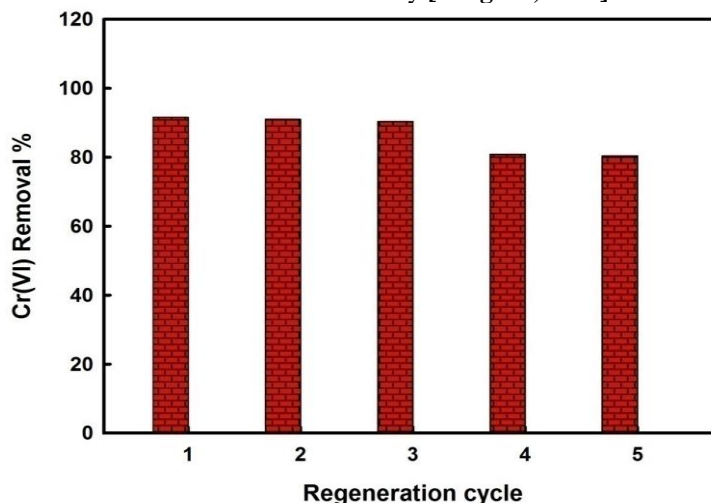


Fig. 16 Regeneration of functionalized of CMNC.

Note that absorption capacity decreased slightly with increased cycles. In the first five cycles, adsorption efficiency of functionalized CMNC remained almost constant : having been refurbished three times, the Cr removal rate was still more than 80%. This fact suggests that functionalized CMNC can be used as a reusable to absorb the Cr adsorption from aqueous.

Conclusions

The Fe_3O_4 magnetic nanoparticles and chitosan magnetic nanocomposite were successfully prepared by chemical co-precipitation technique and Ex situ process respectively. Amination of CMNC with hexamine to get functionalized CMNC revealed a significant effects for Cr(VI) removal in wider range of pH. The characterization results of the prepared Fe_3O_4 magnetic nanoparticles, CMNC and functionalized CMNC was confirmed the composition, structure and the thermal

stability of each prepared samples. The adsorption results show that the functionalized CMNC possessed high activity for Cr(VI) removal in any condition of acidic, neutral and basic solutions with the percentage sorption of chromium reached to 91.7%. The sorption isotherms fitted with the Langmuir, Freundlich and Temkin models show that the Freundlich isotherm model had the best fit with $R^2=0.9974$ with functionalized CMNC. The kinetic data for Cr(VI) sorption with functionalized CMNC was found that fitted well with the pseudo-second order kinetic model. The functionalized CMNC reuse indicates that the adsorbents have an absorption capacity higher than 80% after five regeneration cycles.

References

- [1]. Auta M. and Hameed B.H, (2014), "Chitosan Clay Composite As Highly Effective and Low Cost Adsorbent For Batch and Fixed Bed Adsorption of Methylene Blue".
- [2]. Dogan M., Abak H. and Alkan M., (2009), "Adsorption of Methylene Blue On To Hazenut Shell".
- [3]. Dong C., W. Chen and C. Liu, (2014), "Preparation of Novel Magnetic Chitosan Nanoparticle and Its Application For Removal of Humic Acid From Aqueous Solution", 1067–1076.
- [4]. Dong Wan Cho, Byong-Hun Jeon, Chul-Min Chon, Yongje Kim, Franklin W. Schwartz, Eung-Seok Lee and Hocheol Song, (2012), "A Novel Chitosan/Clay/Magnetite Composite For Adsorption of Cu(II) and As(V)". *Environ. Manage.* 91, 798–806.
- [5]. Freundlich H.M.F., (1906), "Over The Adsorption In Solution", *J. Phys. Chem.*, Pp. 385-471.
- [6]. George Z. Kyzas and Eleni A. Deliyanni, (2013), "Mercury(II) Removal With Modified Magnetic Chitosan Adsorbents".
- [7]. Hong Li, (2016), "Global Trends & Challenges In Water Science, Research and Management", Second Edition, 4.
- [8]. Hua Yue Zhu, Ru Jiang and Ling Xiao, (2010), "Adsorption of An Anionic Azo Dye By Chitosan/Kaolin/ Γ -Fe₂O₃ Composites".
- [9]. Jucely Dos Santos Menegucci, Mac-Kedson Medeiros Salviano Santos, Diego Juscelino Santos Dias, Juliano Alexandre Chaker and Marcelo Henrique Sousa, (2015), "One-Step Synthesis of Magnetic Chitosan For Controlled Release of 5-hydroxytryptophan".
- [10]. Katayoon Kalantari, Mansor B. Ahmad, Kamyar Shameli, Mohd Zobir Bin Hussein, Roshanak Khandanlou, and Hajar Khanehzaei, (2014), "Size-Controlled Synthesis of Fe₃O₄ Magnetic Nanoparticles in the Layers of Montmorillonite".
- [11]. Khalid Z. Elwakeel, (2010), "Removal of CR(VI) From Alkaline Aqueous Solution Using Chemically Modified Magnetic Chitosan Resins", New Cairo City, Egypt.
- [12]. Kyzas, G.Z., and Lazaridis, (2009), "Reactive and basic dyes removal by sorption onto chitosan derivatives", *J. Colloid Interface Sci.* 331(1), 32-3.
- [13]. Langmuir Irving, (1916), "The Constitution and Fundamental Properties of Solids and Liquids Part I. Solids".
- [14]. Nguyen Ngoc Thinh, Pham Thi Bich Hanh, Le Thi Thanh Ha, Le Ngoc Anhc, Tran Vinh Hoang, Vu Dinh Hoang, Le Hai Dang and Nguyen Van Khoi, (2012), "Chitosan–Magnetite Nanoparticles For Removal of Cr(VI) From Aqueous Solution".
- [15]. Peng Wang, Tingguo Yan and Lijuan Wang, (2013a), "A Novel Chitosan/Clay/Magnetite composite For Adsorption of Cu(II) And As(V)".
- [16]. Peng Wang, Tingguo Yan and Lijuan Wang, (2013b), "Removal of Congo Red From Aqueous Solution Using Magnetic Chitosan Composite Microparticles", 6029.
- [17]. Pooja Singh and R. Nagendran, (2013), "A Comparative Study of Sorption of Chromium (III) Onto Chitin and Chitosan".
- [18]. Shahriar Mahdavi, Mohsen Jalali and Abbas Afkhami, (2012), "Removal of Heavy Metals From Aqueous Solutions Using Fe₃O₄, ZnO, and CuO Nanoparticles".
- [19]. Temkin, M.J. and Pyzhev V., (1940), "Recent Modifications To Langmuir Isotherms", *Acta Physiochim. USSR* 12: 217-222.
- [20]. Thinh N.N., P.T.B. Hanh, L.T.T. Ha, L.N. Anh, T.V. Hoang and V.D. Hoang, (2013), "Magnetic Chitosan Nanoparticles For Removal of Cr(Vi) From Aqueous Solution", 1214–8.
- [21]. Vaishnavi S., Sureshkumar, C. Kiruba G. Danie, Ruckmani K. and Sivakumar M., (2015), "Fabrication of Chitosan–Magnetite Nanocomposite Strip For Chromium Removal".
- [22]. Waldon RD, (2008), "Infrared Spectra of Ferrites", *J Phys Rev*, 1955(99):1727.
- [23]. Xin Jiang Hu, Jing-Song Wang, Yun-Guo Liu, Xin Li, Guang-Ming Zeng, Zheng-Lei Bao, Xiao-Xia Zeng, An-Wei Chen and Fei Long, (2010), "Adsorption of Chromium (VI) By Ethylenediamine-Modified Cross-Linked Magnetic Chitosan Resin: Isotherms, Kinetics and Thermodynamics".